

NJC

Accepted Manuscript



This is an *Accepted Manuscript*, which has been through the Royal Society of Chemistry peer review process and has been accepted for publication.

Accepted Manuscripts are published online shortly after acceptance, before technical editing, formatting and proof reading. Using this free service, authors can make their results available to the community, in citable form, before we publish the edited article. We will replace this *Accepted Manuscript* with the edited and formatted *Advance Article* as soon as it is available.

You can find more information about *Accepted Manuscripts* in the [Information for Authors](#).

Please note that technical editing may introduce minor changes to the text and/or graphics, which may alter content. The journal's standard [Terms & Conditions](#) and the [Ethical guidelines](#) still apply. In no event shall the Royal Society of Chemistry be held responsible for any errors or omissions in this *Accepted Manuscript* or any consequences arising from the use of any information it contains.

ARTICLE

Fabrication of Functionalized SiO₂/TiO₂ Nanocomposites via in Amidation for the Fast and Selective Enrichment of Phosphopeptides

Cite this: DOI: 10.1039/x0xx00000x

Received 00th January 2012,
Accepted 00th January 2012

DOI: 10.1039/x0xx00000x

www.rsc.org/

¹⁰Yue Hu, Chen Xiao Shan, Jun Wang, Jun-Ming Zhu, Chao-Qian Gu, Wen-Ting Ni, Dong Zhu* and Ai-Hua Zhang*

Only single-functionalized nanomaterials could not fully meet the requirement of biological applications, although most of them have been still applied for the enrichment of phosphopeptides. Multifunctional nanocomposites provided multiple specific enrichment capacity for phosphopeptides is becoming new research focus. Here, a simplified and effective system was developed for the fast and highly selective enrichment of phosphopeptides using functionalized SiO₂/TiO₂ nanocomposites as sorbents. The functionalized SiO₂/TiO₂ nanocomposites were prepared by the amidation between amino groups of mesoporous SiO₂ nanoparticles and carboxyl groups of TiO₂ nanocrystals, which make the nanocomposites' surface possess highly absorption for phosphopeptides taking advantage of both strong anion exchange of amine-functionalized SiO₂ nanospheres and high metal oxide affinity of TiO₂ nanocrystals. A simplified approach using a pipet tip filled with prepared functionalized SiO₂/TiO₂ nanocomposites was applied to enrich phosphopeptides from digests of phosphoprotein (β -casein), protein mixtures of β -casein and bovine serum albumin (BSA) and the nonfat milk. In this approach, phosphopeptides were rapidly enriched from the digested peptides in less than one minute. Using phosphopeptides analysis by MALDI-TOF-MS, the limit of detection for phosphopeptides was able to reach approximately 10 femtomoles. With highly selective enrichment efficiency, the functionalized SiO₂/TiO₂ nanocomposites would hold great promise for applications in MS-based phosphoproteomics.

Introduction

Protein reversible phosphorylation is regarded as the most common post-translational modification in the regulation of cellular activities,¹⁻³ which thus participates in varieties of regulatory functions such as cell growth, division, proliferation, and signal transduction.⁴⁻¹⁰ At present, mass spectrometry especially matrix-assisted laser desorption/ionization time-of-flight mass spectrometry (MALDI-TOF-MS) is usually applied to characterize phosphoproteins.¹¹⁻¹² However, the direct MS analysis of phosphorylated peptides from digestion samples seriously subjects to the stoichiometric trouble of phosphorylation as well as the ion suppression by the abundant

College of Pharmacy, Nanjing University of Chinese Medicine, Nanjing 210023, P. R. China.

E-mail: dongzhunjutcm@hotmail.com; aihuazhang_5912@163.com;

Fax: +86 2585811839; Tel: +86 2585811839

Electronic supplementary information (ESI) available: See DOI: 10.1039/b000000x/

coexistence of nonphosphopeptides. Moreover, the analysis of phosphopeptides also suffers from the low ionization efficiency and limited detection sensitivity under mass spectrometric conditions.¹³⁻¹⁵ Therefore, the selective enrichment of phosphopeptides from the complex samples is essential before MS analysis.

In recent decades, plenty of pre-treatment techniques have been applied to the enrichment of phosphopeptides¹⁶⁻¹⁸ including covalent chemical modification,¹⁹ immobilized metal affinity chromatography (IMAC),²⁰⁻²² and metal oxide affinity chromatography (MOAC).²³⁻²⁷ MOAC is generally as one of the most widespread enrichment approaches for its higher selectivity upon phosphopeptides trapping, based on bidentate interactions between metal oxides such as TiO₂ and phosphate groups²⁸⁻²⁹.

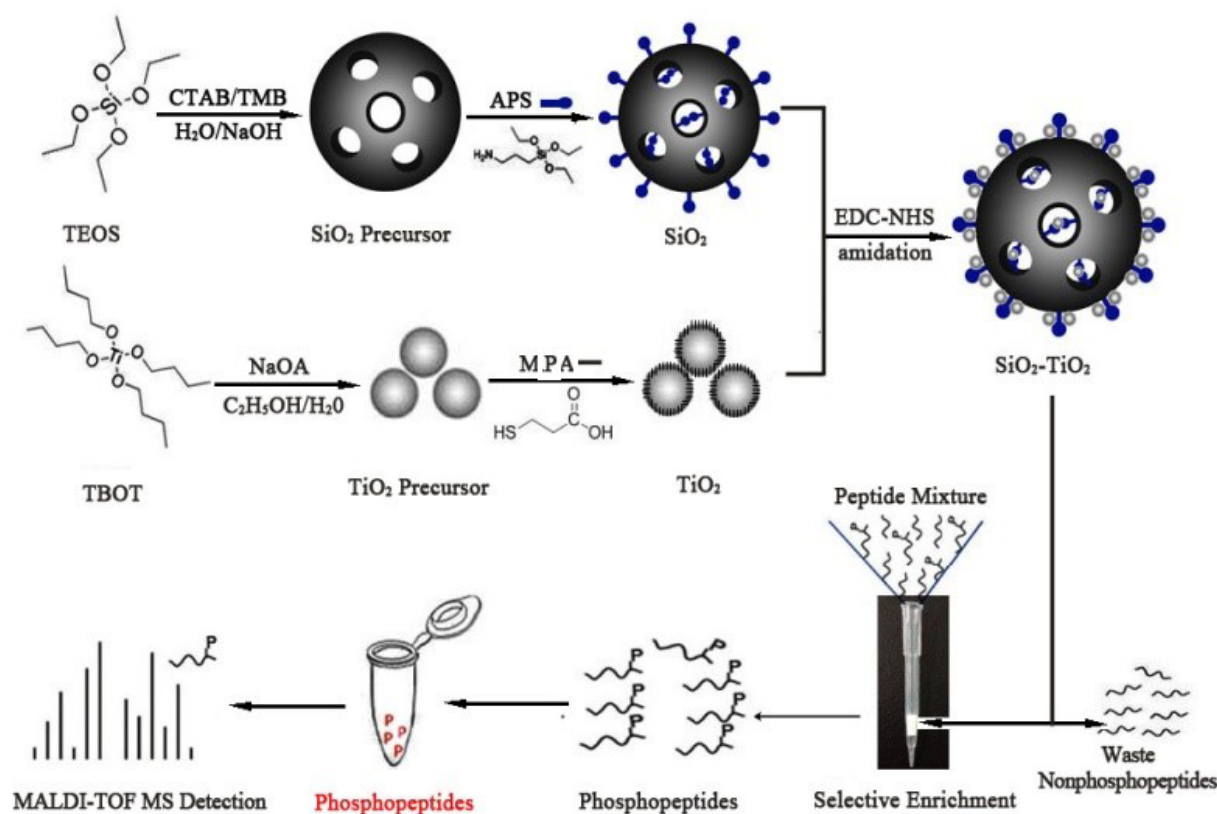
However, pure TiO₂ shows quite strong interaction between multi-phosphopeptides and them owing to the strong Lewis acidity on the surface of TiO₂, which induces to irreversibly absorb phosphopeptides.³⁰⁻³⁴ Meanwhile, mesoporous nanostructured SiO₂ sorbents have already been explored to

enhance loading capacity and enrichment efficiency of analytes.³⁵⁻⁴⁰ SiO₂/TiO₂ nanocomposites have been proved to have better performance on the enrichment of phosphopeptides, resulting from their properties including interfacial electronic properties, structural interactions, as well as appropriate Lewis acidity.^{30, 41-46} Most nanocomposites of SiO₂-TiO₂ created so far have been prepared by either the surface sol-gel process or by a molecular layer-by-layer self-assembly technique.⁴⁷ However, the surface sol-gel process is difficult to control, and inevitable coating cracks are usually produced during the process, while the molecular layer-by-layer self-assembly technique requires special pre-existing molecular recognition condition, which is limited in its application.⁴⁷ Therefore, the development of a steady composite technique possessed stable and firmly bond is critical for the further enrichment of phosphopeptides.

On the other hand, centrifugation is a common step in the extraction procedure of the selective enrichment of phosphopeptides by absorbents material. However, some shortcomings still existed such as time-consuming, coprecipitation of unwanted interferences and/or loss of some target analytes. In this regard, a fast, convenient and effective pretreatment procedure is highly needed to avoid or decrease the

degradation of endogenous phosphoproteins by proteases released ex vivo during the treatment.

In this study, functionalized SiO₂/TiO₂ nanocomposite were prepared via the amidation between amino groups of mesoporous SiO₂ nanoparticles and carboxyl groups of TiO₂ nanocrystals to fast and selectively enrich phosphopeptides as shown in Scheme 1. The successful bond of TiO₂ nanocrystals with SiO₂ nanospheres was confirmed by transmission electron microscopy (TEM), energy-dispersive X-ray spectrum (EDX), Fourier transform infrared (FT-IR). The mesoporous nanocomposites could provide highly selective enrichment for phosphopeptides owing to combine both metal-phosphate ion-pair interactions from TiO₂ and strong anion exchange of SiO₂ nanospheres. A simplified approach using a pipet tip filled with mesoporous SiO₂/TiO₂ nanocomposites was applied to enrich phosphopeptides from digests of phosphoprotein (β -casein), protein mixtures of β -casein and bovine serum albumin (BSA) and the nonfat milk. Enrichment of phosphoprotein was achieved in a very short time (less than one minute) at approximately 10 femtomoles.



Scheme 1. The synthesis procedure for SiO₂ nanospheres, TiO₂ nanocrystals; the preparation of mesoporous SiO₂/TiO₂ nanocomposite and its application in the fast and highly selective enrichment of phosphopeptides.

Experimental section

Chemicals

3-Mercaptopropionic acid (MPA) was purchased from Fluka. 1-(3-Dimethylaminopropyl)-3-ethylcarbodiimide hydrochloride (EDC), N-Hydroxysuccinimide (NHS), N-cetyltrimethyl ammonium bromide (CTAB), tetraethyl orthosilicate (TEOS), mesitylene (TMB), and 3-Aminopropyltriethoxysilane (APS) were obtained from Aladdin. Other chemicals were purchased from the Shanghai Reagent Company. The nonfat milk was acquired from a local supermarket. All these reagents were analytical and used as-received without further treatment. Purified water prepared for all experiments was obtained from milli-Q-RO4 water purification system. (Millipore Simplicity MA, USA)

Apparatus and characterization

Transmission electron microscopy (TEM) images were recorded on a JEOL JEM-2010 CX with an accelerating voltage of 100 kV. The chemical composition of the SiO₂-TiO₂ composites was examined by a Shimadzu EDX-720 energy-dispersive X-ray (EDX) spectrometer (Kyoto, Japan) using Mg Ka radiation as the excitation source. X-ray diffraction (XRD) measurements were performed on a Shimadzu XRD-6000 powder X-ray diffractometer, using Cu Ka as the incident radiation. The surface analysis was performed by nitrogen sorption isotherms at 77 K with a micromeritics ASAP2020 sorptometer. The surface areas were calculated by the Brunauer–Emmett–Teller (BET) method, and the pore size distributions were calculated by the Barrett–Joyner–Halenda (BJH) method. The measurement of the infrared spectroscopy was performed using a Nicolet IR100 infrared spectrometer. Thermo-gravimetric analysis (TGA) was performed on a NETZSCH STA 449 C TGA instrument at a heating rate of 20 °C min⁻¹ in a nitrogen flow from 100 to 750 °C. UV-vis absorption spectra were obtained by a UV-3600 spectrophotometer (Shimadzu).

Preparation of Mesoporous SiO₂/TiO₂ Nanocomposite

The synthesis procedure for SiO₂ nanospheres is shown in Scheme 1. SiO₂ nanospheres were synthesized in one pot via a hydrothermal route, similar to previous report.⁴⁸ Briefly, CTAB (1.0 g) and TMB (7.0 mL) were successively added into a solution containing deionized water (480 mL) and 3.5 mL of 2 mol/L NaOH (aq), followed by vigorous stirring at 80 °C for 4 h. Then, TEOS (5 mL) was quickly added into the mixture under the same reaction conditions for another 2 h. The resultant precipitate was treated by filtration, washing with copious ethanol, and drying overnight in a vacuum at 45 °C. Importantly, dried precipitate needed to be refluxed in ethanol solution of ammonium nitrate (NH₄NO₃/C₂H₅OH, 10mg/mL) to remove the structure-template CTAB and TMB. For the sake of surface modification, the obtained products were functionalized with amino groups of APS within anhydrous ethanol at 80 °C for 6 h. Subsequently, the reaction mixture was treated by centrifugation, washing with ethanol for several times, and drying overnight in a vacuum at 45 °C for 12 h to give mesoporous SiO₂ nanocrystals.

The synthesis of TiO₂ nanocrystals can also be seen in Scheme 551. The detailed steps are as follow⁴⁹: 2.0 g of sodium oleate (NaOA) was dispersed in the mixed solution of 15 mL of absolute ethanol and 10 mL of deionized water, followed by slowly adding 1.0 mL of tetrabutyl titanate (TBOT) and treating with vigorous stirring for 15 min. The hydrolysis and 60 condensation reaction was performed in closed container at 150 °C for 12 h. After washing with deionized water and ethanol, TiO₂ composite precursor (100 mg) was mixed in 20 mL of dichloromethane (DCM). Then, 200 uL of 3-mercaptopropionic acid (MPA) was added into the mixture. The reaction was 65 vigorously stirred at room temperature for 2 h. The resultant products were collected, washed, and dried to give TiO₂ nanocrystals as white powder. The fabrication for mesoporous SiO₂/TiO₂ nanocomposite is shown in Scheme 1 too. Both amino groups of mesoporous SiO₂ nanospheres and carboxyl groups of 70 TiO₂ nanocrystals in virtue of surface modification were mixed (m/m 10:4) in deionized water before activated by crosslinking agent (EDC-NHS), followed by vigorous stirring at 30 °C for 2 h. The products were filtrated and dried in a vacuum at 45 °C for 12 h to obtain resultant nanocomposite as white powder.

Applications in Enrichment of Phosphopeptides

Tryptic Digests of Proteins. β-caseins (1mg/mL, 1mL) were mixed with trypsin (0.05 mg/mL, 1 mL) in ammonium bicarbonate solution (50 mM, pH 8.0) and incubated at 37 °C for 24 h. Digests were stored at -20 °C prior to enrichment processes. 80 BSA (1.0 mg) and the nonfat milk (1 mL) were additionally first denatured by mixing with an aqueous solution (1 mL) containing ammonium bicarbonate (50 mM) and urea (8 M) at 56 °C for 30 min, and 50 μL of the above mixture reduced with 50 μL of 10 mM 1,4-dithiothreitol (DTT) at 56 °C for 1 h. 50 μL of the 85 reduced cysteine residues were alkylated with 50 μL of 20 mM iodoacetamide (IAA) at room temperature and the resulting mixture was incubated for an additional 30 min in the dark prior to the enzymatic digestion. Then, the urea content of solution was 2 M prior to the trypsin digestion to minimize the impact of 90 urea on trypsin activity. Prior to extraction, all the peptide mixtures were diluted to a certain concentration with 50% (v/v) acetonitrile containing 0.1% TFA aqueous solution.

Enrichment of Phosphopeptides Using a Pipet Tip Filled with SiO₂/TiO₂ Nanocomposite. The carrier loaded with materials 95 developing for phosphopeptides enrichment is sterile pipet tips with a capacity of 0.1–20 μL and glass wools used in the pipet tip as a stopper (Scheme 1). Firstly, enrichment materials were tightly placed in a 10 μL pipet tip with glass wool on both sides, while digested protein samples were aspirated into the pipet tip. 100 After 10 s, the solution was dispensed out of the tip. Secondly, the materials with captured peptides in the pipet tip were washed for three times using 10 μL 100 mM acetate buffer: ACN mixture (v/v, 4:1) at pH 4.0 to remove the nonspecific adsorbed peptides. And then, the trapped samples were directly eluted with 10 μL 105 of desorption solution (1:1 (v/v) ACN: water containing 1% (v/v) TFA) at pH 1.0. At last, 1 u L of mixture and 1 μL of matrix solution (20 mg/mL DHB in 50% ACN containing 1% H₃PO₄) was deposited onto the MALDI target for further MS analysis.

MALDI Mass Spectrometry. All MALDI-TOF-MS spectra were recorded with Axima TOF2 mass spectrometry (Shimadzu, Kyoto, Japan). The instrument was equipped with a 337 nm nitrogen laser with a 3 ns pulse width. The detection was performed in positive ion reflector mode with an accelerating voltage of 20 kV. Typically, 200 laser shots were averaged to generate each spectrum. Afterwards, 1 μ L of samples was directly spotted onto the MALDI plate, while 1 μ L of matrix solution (20 mg/mL DHB in 50% ACN containing 1% H_3PO_4) was added to the sample spot. Along with air drying of each spot, peptide mass mapping was carried out.

Results and Discussion

Characterization of Functionalized SiO_2/TiO_2 Nanocomposites

The functionalized SiO_2/TiO_2 nanocomposites were characterized by transmission electron microscopy (TEM) as shown in Figure 1. Figure 1A shows that mesoporous SiO_2 nanospheres were uniform spherical nanoparticles with a mean diameter of approximately 100 nm. The distinct contrast within the SiO_2 nanospheres was derived from the difference in electron density, indicating that the nanospheres exhibit a mesoporous structure. The prepared TiO_2 nanoparticles were about 5 nm as shown in Figure 1B. After the amidation between the amino groups of SiO_2 and the carboxyl groups of TiO_2 , highly integrated mesoporous SiO_2/TiO_2 nanocomposite could be clearly seen in Figure 1C, which shows high specific surface area due to mesoporous nanostructure, indicating that SiO_2/TiO_2 possessed superiority to capture phosphopeptides.

The nanocomposites were also analyzed by X-ray energy dispersive spectroscopy (EDS) as shown in Figure 1(D). The analysis data showed that the ratio of Ti/Si is 36.43/20.50 (wt%). The lack amount of oxygen can be attributed to the limited detection sensitivity for O.

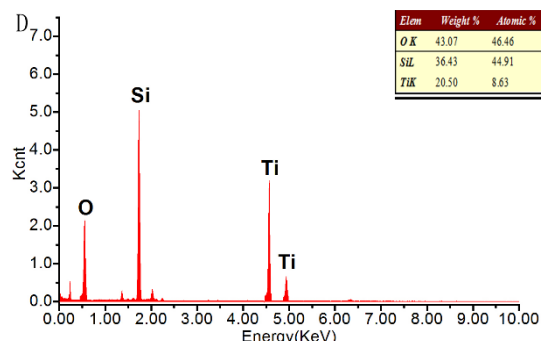
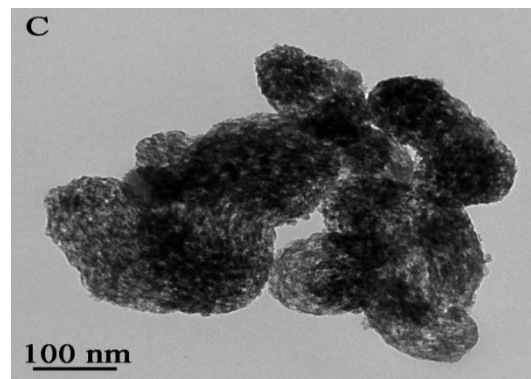
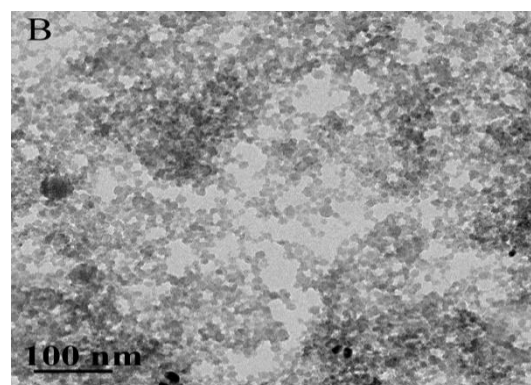
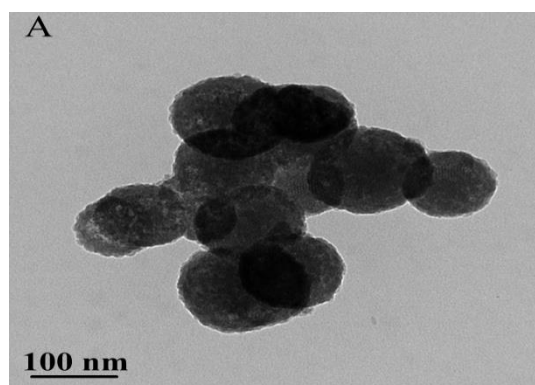


Figure 1. TEM images of mesoporous SiO_2 (A), TiO_2 (B), and SiO_2/TiO_2 nanocomposite (C) and the EDX spectrum (b) and chemical composition (the insert table) of the SiO_2-TiO_2 composites. The wt% and at% in the inset table referred to the weight and atom percentage, respectively. (D)

As shown in Figure 2(A), the X-ray diffraction spectrum of pure SiO_2 produced a single broad signal demonstrating its amorphous state. In contrast, SiO_2/TiO_2 nanocomposites produced several sharp peaks, which represents a high degree of crystalline structure of TiO_2 nanoparticle. By using Scherrer's formula, the grain size of titania particles on SiO_2/TiO_2 was estimated to be ~ 4 nm, which is in good agreement with the TEM result.

The BET isotherms of the pure SiO_2 nanospheres and SiO_2/TiO_2 nanocomposites (Fig. 2(B)) both exhibited the characteristic type of I-V curves with a hysteresis loop generated by capillary condensation according to the IUPAC classification, which indicated that both of them possess uniform porous channels. Despite that the adsorbed nitrogen amount of SiO_2/TiO_2 nanocomposites was reduced respectively, the shape of the hysteresis loop remained unchanged, which indicated that the

pore shape was not significantly changed after successively grafting with TiO₂. The specific surface area and pore volume of pure SiO₂ were determined to be about 607 m² g⁻¹ and 0.64 cm³ g⁻¹, respectively. After bonding with TiO₂ nanoparticle via *in situ* amidation subsequently, the surface area of the SiO₂/TiO₂ nanocomposites were decreased to 313 m² g⁻¹, and the corresponding pore volume were also decreased to 0.42 cm³ g⁻¹. The relatively large surface area and pore volume strongly support the fact that the nanospheres have a porous structure, which is attractive for loading phosphopeptides.

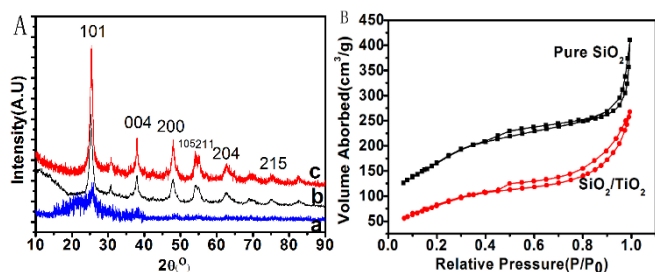


Figure 2 (A). XRD patterns for the pure SiO₂ nanospheres (a), pure TiO₂ (b) and SiO₂/TiO₂ nanocomposites (c). (B). N₂ adsorption-desorption isotherms of pure SiO₂ nanospheres and SiO₂-TiO₂ nanocomposites.

The bond of TiO₂ nanoparticles onto the SiO₂ nanospheres was further confirmed by the FT-IR spectra as shown in Figure 3. In the spectra of SiO₂, the broad adsorption peak in the range of 3700-3200 cm⁻¹ was due to the stretching vibration of N-H and O-H. After the amide reaction with TiO₂, the new absorption bands were observed at 2923 and 2852 cm⁻¹, which could be assigned to the stretching vibration of -C-H of methyl and methylene attributed to crosslinking agent (EDC-NHS). Moreover, a peak assigned to N-H asymmetric bending vibration at 1470 cm⁻¹ and adsorption peaks assigned to C=O stretching vibration in the amido bond at 1640 cm⁻¹, confirmed the successful amidation between SiO₂ and TiO₂.

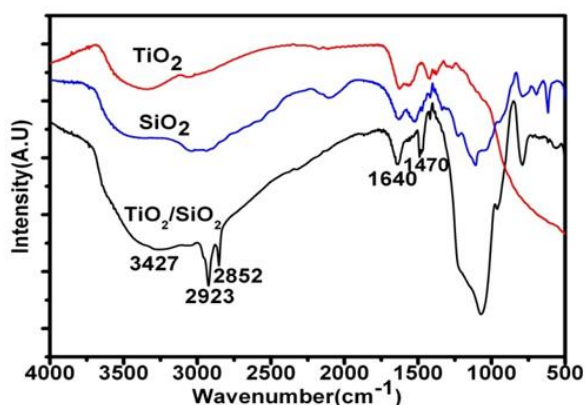


Figure 3. FT-IR pattern of SiO₂, TiO₂, and SiO₂/TiO₂ nanocomposites.

Fast and Highly Selective Enrichment of Phosphopeptides

Derived from Standard Proteins

The mass spectra of tryptic digests of β -casein without enrichment and after enrichment using different materials are shown in Figure 4. The phosphopeptides' signals of direct β -casein analysis were severely suppressed by the dominated nonphosphopeptides (Figure 4A). After enrichment with TiO₂ nanoparticles and SiO₂/TiO₂ nanocomposites with different atom ratio of Ti/Si (Figure 4 B, C, D, E respectively), at least part of phosphopeptides can be successfully captured. In the case of pure TiO₂ nanoparticles, single phosphorylated peptides take a majority place in the mass spectrum (Figure 2B), and the multi-phosphopeptides signal (*m/z* of 3123.2) is very weak compared with SiO₂/TiO₂ nanocomposites. Compared with the SiO₂/TiO₂ nanocomposites with 0.09 and 0.27 atom ratio of Ti/Si, the nanocomposites with Ti/Si of 0.19 shows a better signal-to-noise ratio and a significantly enhanced affinity for both mono-phosphopeptides and multi-phosphopeptides. In Figure 4D, signals of doubly charged [M+2H]²⁺ molecular ions for β 1, β 2, and β 4 phosphopeptides were also observed in the mass spectrum. Four specific phosphopeptides identified with reformative signal intensities are listed in Table 1.

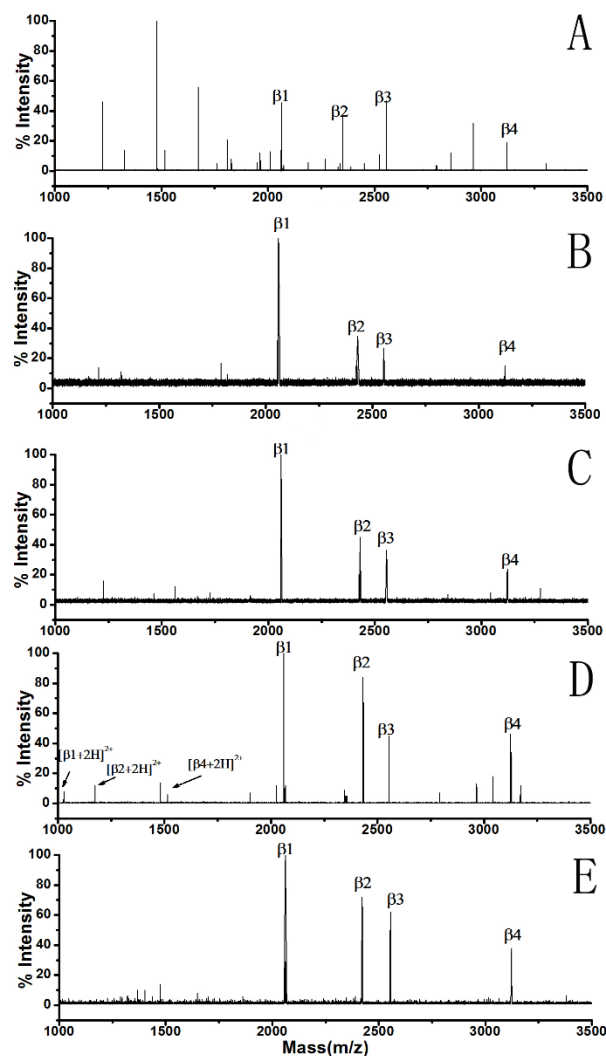


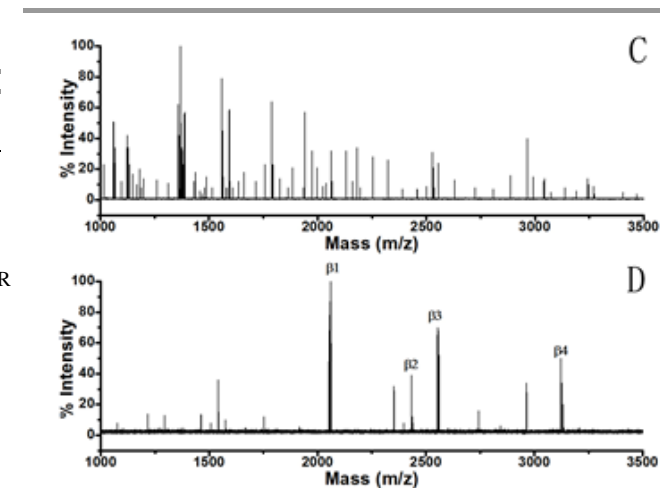
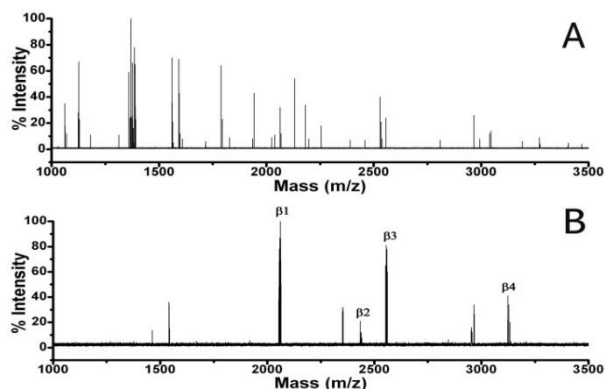
Figure 4. MALDI-TOF mass spectra of the tryptic digests of β -casein obtained by: without enrichment (A), after enrichment using pure TiO₂ (B) and after enrichment

using SiO₂/TiO₂ with 0.09 (C), 0.19 (D), 0.27 (E) atom ratio of Ti/Si. Phosphopeptides are marked with “βn” listed in Table 1.

Table 1. Supporting Information of Identified Phosphopeptides from Tryptic Digest of β-casein

protein	[M+H] ⁺	amino acid sequence
β1	2061.978	FQS*EEQQTEDELQDK
β2	2432.220	IEKFQS*EEQQTEDELQDK
β3	2555.576	FQS*EEQQTEDELQDKIHPE
β4	3123.218	RELEELNVPGEIVES*LS*S*S*EESITR

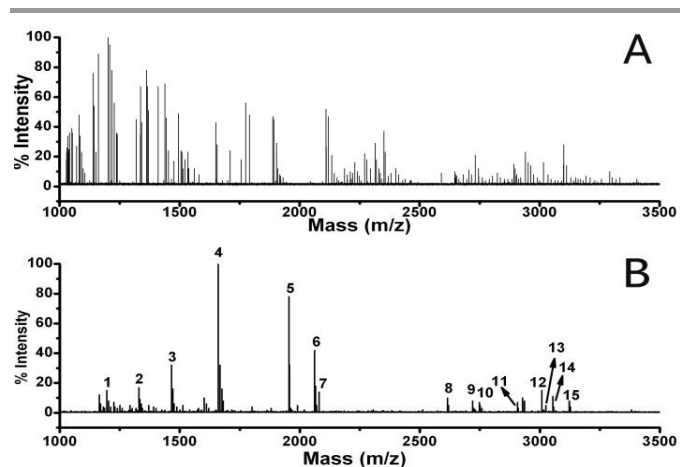
5 To further evaluate the selectivity enrichment of the SiO₂/TiO₂ nanocomposites for the phosphopeptides in the presence of a huge amount of nonphosphopeptides, tryptic digest of BSA was added to the tryptic digests β-casein at a 50:1 and 150:1 mole ratio (BSA : β-casein at the same amount as before) to increase
10 the complexity of the samples. A solution of β-casein phosphopeptides (each 0.87 nmol) was prepared in 100 μL of certain concentration with 50% (v/v) acetonitrile (containing 0.1% (v/v) TFA). This solution was diluted to 200 fmol/μL prior to adding into the tryptic digest of BSA. This mixture of
15 phosphopeptides (4 fmol/μL) and the tryptic digest of BSA (phosphopeptides/BSA, 1:50 or 1:150 in mole) was incubated with 10 mg of SiO₂/TiO₂ nanocomposites in a batch experiment. Along with the increase of the BSA digestion, the signals of non-phosphopeptides were significantly enhanced and the signals of
20 phosphopeptides became invisible. As shown in Figure 5 (A) and 5 (C), most signals of phosphopeptides were concealed in the large amounts of nonphosphopeptides in the mixture, and thus the identification of phosphopeptides become especially difficult. Nevertheless, the intense signal of nonphosphopeptides was
25 greatly reduced after enrichment by the SiO₂/TiO₂ nanocomposites, as shown in Figure 5(B) and 5 (D), all the specific phosphopeptides of β-casein could be distinctly observed with desired intensities. The sequence information of these phosphopeptides was listed in Table 1. These results
30 indicated the excellent selectivity of the SiO₂-TiO₂ nanocomposites towards phosphopeptides even in the presence of a large amount of interfering non-phosphopeptides.



35 **Figure 5.** MALDI-TOF mass spectra of the tryptic digests mixture of β-casein and BSA: (A) direct analysis and (B) analysis after enrichment using SiO₂/TiO₂ with a molar ratio of β-casein to BSA of 1:50, (C) direct analysis and (D) analysis after enrichment using SiO₂/TiO₂ with a molar ratio of β-casein to BSA of 1:150. Phosphopeptides are marked with “βn” listed in Table 1.

40 Fast and Highly Selective Enrichment of Phosphopeptides Derived from Nonfat Milk

Phosphopeptide enrichment efficiency of the functionalized SiO₂/TiO₂ nanocomposites was also tested using nonfat milk that was the typical complex samples to follow the capability of the
45 nanocomposites. Nonfat milk was digested by trypsin after the reducing all proteins in the milk and then phosphopeptide enrichment procedure onto the nanocomposites was applied. Positive ion and linear mode MALDI-MS spectrum of the digested nonfat milk before the phosphopeptide enrichment was
50 obtained as shown in Figure 6(A). Also the enrichment of the phosphopeptides using digested nonfat milk sample onto the functionalized SiO₂/TiO₂ nanocomposites was carried out and the MALDI-MS spectrum of the sample after enrichment is given in Figure 6(B). In Figure 6(A), the dominant signals of
55 nonphosphopeptides severely interfered with the identification of phosphopeptides, while the signals of species other than the phosphopeptides could be greatly reduced as shown in Figure 6(B). All phosphopeptides found in the nonfat milk are given in Table 2. Obviously, it could be concluded that the prepared
60 mesoporous SiO₂/TiO₂ nanocomposite has remarkable selectivity for the enrichment and specific purification of phosphopeptides the enrichment in more complex materials.



the nonfat milk: (A) direct analysis and (B) analysis after enrichment using $\text{SiO}_2/\text{TiO}_2$. Numbers indicate the identified tryptic peptide fragments of nonfat milk digests listed in Table 2.

Figure 6. MALDI-TOF mass spectra of peptides derived from

Table 2. Identified Phosphopeptides Obtained from Tryptic Digest of the Nonfat Milk Enriched by $\text{SiO}_2/\text{TiO}_2$ Nanocomposite.

peak label	$[M+H]^+$	phosphorylation site	protein	amino acid sequence
1	1197.218	1	α S2-casein	KNMAINPS*KENL
2	1330.652	2	α S2-casein	EQLS*TS*EENSK
3	1466.317	1	α S2-casein	TVDMES*TEVFTK
4	1660.784	1	α S1-casein	VPQLEIVPNS*AEER
5	1954.576	1	α S1-casein	YKVPQLEIVPNS*AEER
6	2061.978	1	β -casein	FQS*EEQQTEDELQDK
7	2080.322	1	α S1-casein	KKYKVPQLEIVPNS*AEERL
8	2616.714	4	α S2-casein	NTMEHVS*S*S*EES*IISQETYK
9	2720.485	5	α S1-casein	QMEAES*IS*S*S*EEIVPNS*VEQK
10	2748.314	4	α S2-casein	NAVPIPTLNREQLS*T*S*EENS*K
11	2907.619	1	α S1-casein	QMEAES*ISSSEEIVPNSVEQKHIQK
12	3008.041	4	α S2-casein	NANEEYSIGS*S*S*EES*AEVATEEVK
13	3025.617	2	α S2-casein	FPQY*LQY*LYQGPIVLNPWDQVKR
14	3054.821	1	β -casein	KKIEKFQS*EEQQTEDELQDKIHFFA
15	3123.516	4	β -casein	RELEELNVPGEIVES*LS*S*S*EESITR

Conclusions

Functionalized $\text{SiO}_2/\text{TiO}_2$ nanocomposites exhibiting multiple enrichment performance was successfully prepared by the amidation between amino groups of mesoporous SiO_2 nanoparticles and carboxyl groups of TiO_2 nanocrystals. They not only have mesoporous structure but also possess excellent trapping capability, which is highly propitious to the fast and highly selective enrichment of phosphopeptides. Moreover, a rapid method based on pipet tips was subsequently developed to enrich phosphopeptide in less than one minute at subpicomole phosphopeptides concentrations. Eventually, nonfat milk as a

more complex sample was also used to examine the efficiency of the $\text{SiO}_2/\text{TiO}_2$ for the phosphopeptide enrichment. Up to 15 phosphopeptides were detectable by MALDI-MS using this novel $\text{SiO}_2/\text{TiO}_2$ nanocomposite filled in a pipet tip. The results demonstrated that they had excellent performance on efficient enrichment of phosphopeptides.

Acknowledgements

We greatly appreciate the National Natural Science Foundation of China for the financial support (21205064). This work was also supported by Fund of State Key Laboratory of Analytical Chemistry for Life Science (SKLACLS1208). We also greatly

appreciate “A Project Funded by the Priority Academic Program Development of Jiangsu Higher Education Institutions” (PAPD).

Notes and References

- M. Chi, Y. Cai, X. H. Qian, *Current Proteomics*, 2010, **7**, 168–176.
- A. Gruhler, J. V. Olsen, S. Mohammed, P. Mortensen, N. J. Faergeman, M. Mann and O. N. Jensen, *Mol. Cell. Proteomics*, 2005, **4**, 310–327.
- G. Redlich, U. M. Zanger, S. Riedmaier, N. Bache, B. M. A. Giessing, M. Eisenacher, C. Stephan, H. E. Meyer, O. N. Jensen and K. Marcus, *J. Proteome Res.*, 2008, **7**, 4678–4688.
- J. V. Olsen, B. Blagoev, F. Gnad, B. Macek, C. Kumar, P. Mortensen and M. Mann, *Cell*, 2006, **127**, 635–648.
- N. C. Tedford, A. B. Hall, J. R. Graham, C. E. Murphy, N. F. Gordon and J. A. Radding, *Proteomics*, 2009, **9**, 1469–1487.
- T. E. Thingholm, O. N. Jensen and M. R. Larsen, *Proteomics*, 2009, **9**, 1451–1468.
- T. E. Thingholm, O. N. Jensen and M. R. Larsen, *Proteomics*, 2009, **9**, 1451–1468.
- Z. A. Knight, B. Schilling, R. H. Row, D. M. Kenski, B. W. Gibson and K. M. Shokat, *Nat. Biotechnol.*, 2003, **21**, 1047–1054.
- B. Fang, E. B. Haura, K. S. Smalley, S. A. Eschrich and J. M. Koomen, *Biochem Pharmacol.*, 2010, **80**, 739–747.
- K. Ashman and Villar, E. L. Clin. *Trans. Oncol.* 2009, **11**, 356–362.
- M. P. Torres, R. Thapar, W. F. Marzluff and C. H. Borchers, *J. Proteome Res.*, 2005, **4**, 1628–1635.
- L. J. Zhang, H. J. Lu, P. Y. Yang and J. Chin, *Anal. Chem.*, 2007, **35(1)**: 146–152
- J. R. Yates, C. I. Ruse, and A. Nakorchevsky, *Annu. Rev. Biomed. Eng.*, 2009, **11**, 49–79.
- F. Tan, Y. Zhang, W. Mi, J. Wang, J. Wei, Y. Cai, and X. Qian, *J. Proteome Res.*, 2008, **7**, 1078–1087.
- B. Bodenmiller, L. N. Mueller, M. Mueller, B. Domon and R. Aebersold, *Nat. Methods.*, 2007, **4**, 231–237.
- A. Leitner, *Trends Anal. Chem.*, 2010, **29**, 177–185.
- L. D. Rogers and L. J. Foster, *Mol. Biosys.*, 2009, **5**, 1122–1129.
- G. Mamone, G. Picariello, P. Ferranti and F. Addeo, *Proteomics*, 2010, **10**, 380–393.
- G. Han, M. Ye and H. Zou, *Analyst*, 2008, **133**, 1128–1138.
- L. H. Hu, H. J. Zhou, Y. H. Li, S. T. Sun, S. T. Guo, M. L. Ye, X. F. Tian, J. R. Gu, S. L. Yang and H. F. Zou, *Anal. Chem.*, 2009, **81**, 94–104.
- X. S. Li, L. D. Xu, G. T. Zhu, B. F. Yuan and Y. Q. Feng, *Analyst*, 2012, **137**, 959–967.
- H. Q. Qin, F. J. Wang, P. Y. Wang, L. Zhao, J. Zhu, Q. H. Yang, R. A. Wu, M. L. Ye and H. F. Zou, *Chem. Commun.*, 2012, **48**, 961–963.
- H. K. Kweon and K. Hakansson, *Anal. Chem.*, 2006, **78**, 1743–1749.
- Y. Zhang, C. Chen, H. Q. Qin, R. A. Wu and H. F. Zou, *Chem. Commun.*, 2010, **46**, 2271–2273.
- J. Y. Yan, X. L. Li, S. Y. Cheng, Y. X. Ke and X. M. Liang, *Chem. Commun.*, 2009, 2929–2931.
- J. H. Wu, X. S. Li, Y. Zhao, W. Zhang, L. Guo and Y. Q. Feng, *J. Chromatogr. A* 2011, **1218**, 2944–2953.
- L. Zhao, H. Q. Qin, Z. Y. Hu, Y. Zhang, R. A. Wu, H. F. Zou, *Chem. Sci.* 2012, **3**, 2828–2838.
- A. Motoyama, T. Xu, C. I. Ruse, J. A. Wohlschlegel and J. R. Yates, *Anal. Chem.*, 2007, **79**, 3623–3634.
- G. Han, M. Ye, H. Zhou, X. Jiang, S. Feng, X. Jiang, R. Tian, D. Wan, H. Zou and Gu, *J. Proteomics.*, 2008, **8**, 1346–1361.
- X. M. He, G. T. Zhu, X. S. Li, B. F. Yuan, Z. G. Shi and Y. Q. Feng, *Analyst*, 2013, **138**, 5495–5502
- L. P. Li, T. Zheng, L. N. Xu, Z. Li, L. D. Sun, Z. X. Nie, Y. Bai and H. W. Liu, *Chem. Commun.*, 2013, **49**, 1762.
- H. K. Kweon and K. Hakansson, *Anal. Chem.*, 2006, **78**, 1743–1749.
- A. Leitner, *TrAC, Trends Anal. Chem.*, 2010, **29**, 177–185.
- F. Wang, C. Song, K. Cheng, X. Jiang, M. Ye and H. Zou, *Anal. Chem.*, 2011, **83**, 8078–8085.
- S. P. Sherlock, S. M. Tabakman, L. M. Xie and H. Dai, *J. ACS Nano*, 2011, **5**, 1505–1512.
- C. A. Nelson, J. R. Szczech, Q. G. Xu, M. J. Lawrence, S. Jin and Y. Ge, *Chem. Commun.*, 2009, **43**, 6607–6609.
- Z. D. Lu, M. M. Ye, N. Li, W. W. Zhong and Y. D. Yin, *Chem. Int. Ed.*, 2010, **49**, 1862–1866.
- J. Y. Yan, X. L. Li, L. Yu, Y. Jin, X. L. Zhang, X. Y. Xue, Y. X. Ke and X. M. Liang, *Chem. Commun.*, 2010, **46**, 5488–5490.
- Z. D. Lu, J. C. Duan, L. He, Y. X. Hu and Y. D. Yin, *Anal. Chem.*, 2010, **82**, 7249–7258.
- A. Mehmet, C. Omur and S. Bekir, *Anal. Chem.*, 2012, **84**, 2713–2710.
- J. Wan, K. Qian, L. Qiao, Y. Wang, J. Kong, P. Yang, B. Liu and C. Yu, *Chemistry-a European Journal* 2009, **15 (11)**, 2504–2508.
- Y. Zhang, C. Chen, H. Qin, R. Wu and H. Zou, *Chemical Communications*, 2010, **46 (13)**, 2271–2273.
- J. H. Wu, X. S. Li, Y. Zhao, W. Zhang, L. Guo and Y. Q. Feng, *Journal of Chromatography A*, 2011, **1218 (20)**, 2944–2953.
- X. M. He, G. T. Zhu and X. S. Li, *ANALYST*, 2013, **138 (18)**, 5495–5502.
- S. T. Wang, M. Y. Wang, X. Su, B. F. Yuan and Y. Q. Feng, *ANALYTICAL CHEMISTRY*, 2012, **84(18)**, 7763–7770
- M. Zhang, F. Wei, Y. F. Zhang, J. Nie and Y. Q. Feng *J. Chromatogr. A* 2006, **1102**, 294–301
- J. H. Wu, X. S. Li, Y. Zhao, W. P. Zhang, L. Guo and Y. Q. Feng, *J. Chromatogr. A*, 2011, **1218**, 2944–2953
- L. Yuan, Q. Q. Tang, D. Yang, J. Z. Zhang, F. Zhang and Jianhua Hu *J. Phys. Chem. C* 2011, **115**, 9926–9932
- X. Wang, J. Zhuang, Q. Peng and Y. D. Li, *NATURE*, 2005, **437**, 121–124